Available online at www.sciencedirect.com
SCIENCE DIRECT®
Physics Letters A 323 (2004) 194–203
PHYSICS LETTERS A
www.elsevier.com/locate/pla

Classification of patterns in excitable systems with lateral inhibition

Bakhtier N. Vasiev

The SIMBIOS Centre, Mathematics Department, Dundee University, Dundee DD1 4HN, UK

Received 24 January 2003; received in revised form 25 November 2003; accepted 15 January 2004

Communicated by A.P. Fordy

Abstract

Propagating waves and stationary spots are widely known solutions for reaction-diffusion systems. Other kinds of patterns, such as pulsating waves and self-replicating spots, have also recently been reported. The aim of this Letter is to examine the parameter space of an excitable system described by modified Fitz-Hugh–Nagumo equations and to classify patterns occurring in one- and two-dimensional media. This permits one to establish certain relations between already known patterns and to discover new patterns such as expanding rings (pulsating or asymptotically stationary) and streaming patterns.

PACS: 05.45.-a; 82.20.Wt; 87.10.+e

Keywords: Excitable system; Pattern formation; Self-replication; Streaming patterns

1. Introduction

A theoretical consideration of many natural systems shows that they can be described by systems of nonlinear reaction–diffusion equations. As a general rule equations forming large systems have significantly different rates of change of variables and this often allows one to reduce the number of equations to two, with these two remaining equations still capturing the main phenomena observed in the original system. On the other hand, depending on the nature and the number of stationary spatially-homogeneous solutions, reaction–diffusion systems can fall into different classes such as excitable (or threshold), oscillatory and trigger (or multistable). Despite the differences between these classes (for example, homogeneous oscillations can be observed only in oscillatory systems while transitions from one steady state to another are only observed in trigger systems) they have a lot in common—solutions such as travelling waves and stationary spots can be observed in all of these systems (with an appropriate set of parameters). In this Letter we focus on patterns arising in two-variable excitable system described by modified Fitz-Hugh–Nagumo equations. We describe all one- and two-dimensional patterns arising in response to a single stimulation and classify them. The results presented can be useful for understanding pattern-formation phe-

E-mail address: bnvasiev@maths.dundee.ac.uk (B.N. Vasiev).
URL: http://www.maths.dundee.ac.uk/~bnvasiev.

0375-9601/$ – see front matter
doi:10.1016/j.physleta.2004.01.068

nomena in hydrodynamic systems, nonlinear optics, autocatalytic chemical reactions and variety of biological systems including excitable tissues (muscles and nerves), developing biological systems (morphogenesis, gastrulation) and many more [1,2].

2. The mathematical model

A general two-variable reaction–diffusion system can be represented as follows:

$$\frac{\partial u}{\partial t} = D_u \Delta u - \epsilon_u f(u, v), \tag{1}$$

$$\frac{\partial v}{\partial t} = D_v \Delta v + \epsilon \phi(u, v), \tag{2}$$

where the functions $f(u, v)$ and $\phi(u, v)$ define the kinetics of the dependent variables u and v, ϵ_u and ϵ specify the rate of kinetics terms and D_u, D_v are diffusion coefficients. For continuous systems, rescaling of time and space allows elimination of one of the diffusion coefficients and one of the ϵ-parameters, so that we can put $D_u = 1$ and $\epsilon_u = 1$ for a rescaled system. Patterns arising in the system (1), (2) with this constrain are studied in Sections 3–5.

Many important systems exhibiting pattern formation are essentially discrete. For example, morphogenetic patterns guiding embryogenesis take place in media formed by cells. The cells are separated from each other by membranes which form considerable barriers for the diffusion of morphogens (normally represented by protein molecules). This implies that in a numerical study of these systems there is a lower bound on the size of the space step used (defined by cell size) and therefore the rescaling of space to scale-out the diffusion coefficient might not be possible. To study discrete patterns we will consider the system (1), (2) with only $\epsilon_u = 1$ and both diffusion coefficients significantly reduced (this is equivalent to a large space step) so that this reflects the discrete nature of the cell systems. The system (1), (2) in this case can be viewed as a coupled map lattice and patterns formed in this system are studied in Section 6.

For this study we use $f(u, v) = k_u u(u - u_0)(u - u_1) + v$ and $\phi(u, v) = u - v$. These kinetics terms are from the so-called Fitz-Hugh–Nagumo (FHN) system, which is a widely known prototype model describing excitable media [3]. The variables of this system can be referred as an activator (u—involved in the increase of its own production) and an inhibitor (v—reduces the production rate of activator). The diffusive spread of the inhibitor around the excited area is often referred to as lateral inhibition [4] (in the standard FHN model $D_v = 0$). k_u, k_v are constants related to the kinetics of the system (e.g., excitable, bistable). For numerical integration of the system (1), (2) we have used the Euler explicit method with central differencing for the diffusion terms and with no-flux conditions on the boundaries of the medium. A set of numerical simulations carried out with various grid sizes and time steps showed that to achieve continuity and accuracy of the solution (while $D_u = 1$) we can set the value of grid size to 0.4 and the time step to 0.01 (or less when $D_v > 4$). Up to a 4-fold reduction of these values always showed less than a 2% change in the velocity of propagating waves, periods and amplitudes of pulsating waves and had negligible effect on the location of boundaries of domains in the parameter space (see Figs. 1, 3). These values of grid size and time step were also used for a numerical integration of the discrete system (when $D_u < 1$). Unless specified otherwise the parameter values used were: $D_u = 1$, $D_v = 4$, $\epsilon = 0.1$, $k_u = 4.5$, $u_1 = 1$, $u_0 = 0.05$.

3. One-dimensional patterns

Stimulation of the medium described by (1), (2) results in the formation of different spatio-temporal patterns. If the inhibitor diffusion is small compared with that of the activator the stimulation causes the formation of propagating waves. If the inhibitor's diffusion is large stationary spots are formed. Patterns forming between these two extremes in a 1D medium were reported in [5]. Generally the parameter space of the system (1), (2) can be divided into four domains (R1–R4) corresponding to four different types of solutions (Fig. 1). R1 is a domain corresponding to propagating wave solutions (Fig. 1A); R2—a domain where the patterns are unstable and the medium as a rule returns to the homogeneous state (Fig. 1B, E); R3—a domain where stable pulsating (or breathing) spots are observed (Fig. 1C); R4—a domain where stationary spots arise (Fig. 1D).

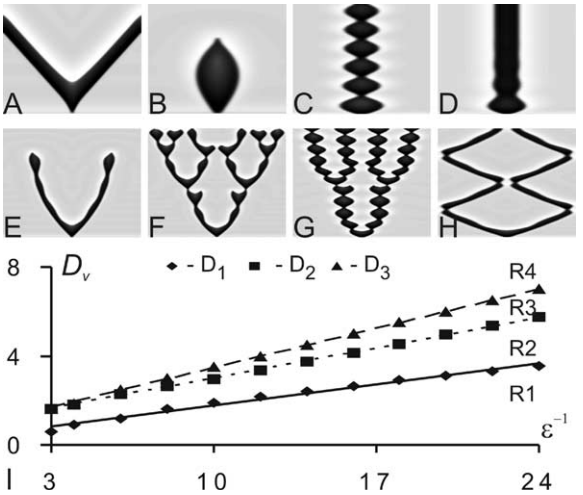

Fig. 1. One-dimensional solutions of the system (1), (2). A–H are time–space plots (time: vertical axis, space: horizontal axis) representing the activator's profile. Patterns are initiated by increasing the levels of u and v in a small area located in the centre of the medium. A: propagating waves (R1 domain on I); C: pulsating spot (R3); D: stationary spot (R4). Solutions in the domain R2: vanishing spot (B) and waves (E), self-replicating waves (F) and spots (G), waves reflecting upon collisions (H). I: location of the domains R1, R2, R3 and R4 on the plane (ϵ^{-1}, D_v). A: size of the plot 100×160, $D_v = 1$; B: 300×240, $D_v = 2$; C: 400×80, $D_v = 3.2$; D: 400×80, $D_v = 5$; E: 100×80, $D_v = 2.7$; F: 400×240, $D_v = 2.1$; G: 1000×240, $D_v = 4.05$, $\epsilon = 16^{-1}$; H: 500×120, $D_v = 1.967$. Note that patterns shown in A–G are not sensitive to the medium size (provided it is large enough) and the size of the plots was varied only for demonstrational purposes.

Spatio-temporal patterns forming in domains R1, R3 and R4 are relatively well known. Only one kind of nontrivial pattern (in response to a single initial stimulation) can be observed in each of them (presented on panels A, C, and D of Fig. 1). However the situation regarding the domain R2 is remarkably different. Different kinds of unstable patterns can be observed there. For example, the pattern presented in Fig. 1E can be classified as an unstable propagating wave [3], while the pattern in Fig. 1B as an unstable pulsating spot. The amplitude of the latter's pulsations is larger than its size and this is the reason why it collapses. This statement is supported by the observation that on the border between the domains R2 and R3 the amplitude of R3-spot pulsations is equal to its (mean) size [5].

In the vicinity of the borders of the R2 domain unstable R2-patterns under some conditions do not decay and become persistent. Examples of these patterns are presented in Fig. 1(F)–(H). Fig. 1F shows a pattern of self-replicating waves while Fig. 1G shows self-replicating spots. Self-replicating waves are observed in the vicinity of the border with the R1 domain while self-replicating spots are observed at the border with the R3 domain. Fig. 1H shows another example of a persistent pattern in the R2 domain formed by waves reflecting upon collisions with each other and the boundaries of the medium. Persistent patterns observed in the R2 domain are not robust. Slight changes in the model parameters, in initial conditions or in the size of medium can dramatically change the overall pattern.

For an analytical estimation of the bifurcation values of D_1 and D_3 let us consider the concentration profiles of u and v in the stationary spot and the propagating wave (Fig. 2B and D). The value v_0 of the inhibitor on the walls of the stationary spot (Fig. 2B) are defined by the condition $\int_{u^-}^{u^+} f(u, v_0)\,du = 0$ where u^- and u^+ are the minimal and maximal roots of the equation $f(u, v_0) = 0$ [6]. Contrary to the stationary spot the profiles of u and v for the propagating wave are not symmetric (Fig. 2D). The link between the values v^+ and v^- of inhibitor on the wave front and back are defined by the condition

$$\int_{u_b^-}^{u_b^+} f(u, v^-)\,du = -\int_{u_{fr}^-}^{u_{fr}^+} f(u, v^+)\,du,$$

where the integration limits are equal to minimal and maximal roots of the corresponding algebraic equations $f(u, v^-) = 0$ and $f(u, v^+) = 0$ [3]. The value v_0 is unique for the given kinetics terms while the values v^+ and v^- can vary and define the velocity of the wave, c.

To simplify our analysis we replace both u-profiles by rectangular functions: $u = 1$ in the excited region and $u = 0$ in the rest of the medium (Fig. 2C and E). This approximation can be justified by the fact that R1–R4 solutions are also observed in the system (1), (2) where $f(u, v)$ is a piecewise linear function [5] such that u-profiles in corresponding solutions are almost rectangular. Now we can derive the analytic expression for the v-profile in a stationary spot by solving the linear equation $D_v v'' + \epsilon(u - v) = 0$ when $u = 1$ for $|x| \leqslant a$ and $u = 0$ for $|x| > a$ with boundary conditions $v(-\infty) = v(\infty) = 0$ as-

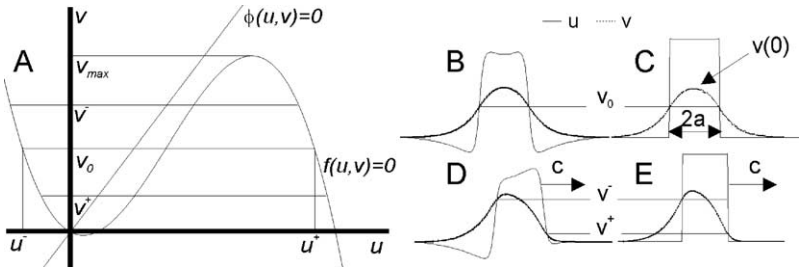

Fig. 2. Null-clines ($f(u,v)=0$ and $\phi(u,v)=0$) of the system (1), (2) are shown in A. The profiles of u (dark) and v (light) for a stationary spot and propagating wave (moving right) are shown in B and D. To simplify the analysis of these solutions profiles of u are replaced by a rectangular function of the excited area, i.e., $u=1$ inside the spot (and the wave) and $u=0$ in the rest of the medium (see C and E). Then v_0 is the value of v on the borders of the stationary spot, v^+ and v^- are the values of v on the front and the back of the wave. Null-cline $f(u,v)=0$ defines the value $v_{\max}$ (A) such that if the value of v exceeds $v_{\max}$ inside the spot or wave, they become unstable and break into pieces [6]. For the function $f(u,v)$ defined in Section 2, $v_0=0.31$, $v_{\max}=0.62$.

suming that $v\in C^1(-\infty,\infty)$ and $v(-a)=v(a)=v_0$. The solution is a symmetric function $v(x)=1+(v_0-1)\cosh(\lambda x)/\cosh(\lambda a)$, for $|x|\leqslant a$ and $v(x)=v_0\exp[\lambda(a-|x|)]$, for $|x|>a$, where $\lambda=\sqrt{\epsilon/D_v}$. The requirement that $v'(x)$ is continuous at $|x|=a$, gives the relationship $a\lambda=0.5\ln(1-2v_0)^{-1}$, i.e., the product $a\lambda$ is constant. Note that the maximum value of inhibitor, $v(0)=1-\sqrt{1-2v_0}$, depends only on v_0. The stationary spot can be initiated provided that this value is smaller than $v_{\max}$ on Fig. 2A [6].

Let us assume that the symmetric variations in the size of the spot and in the value of the inhibitor on the spot's "wall" affect each other according to the system $da/dt=b_{11}\delta a+b_{12}\delta v$ and $dv/dt=b_{21}\delta a+b_{22}\delta v$. The stationary spot is stable if for the Jacobian matrix B, associated with this system, $\det(B)>0$ and $\operatorname{tr}(B)<0$. Since $D_v=D_3$ corresponds to the stationary–pulsating spot transition, this bifurcation point is associated with $\operatorname{tr}(B)=b_{11}+b_{22}=0$. For b_{11}, we can write $b_{11}=c'(v_0)v'(a)$ where $c(v)$ is a velocity of the spot's "wall" as a function of the inhibitor concentration. The derivative $c'(v)$ is negative (c increases with a decrease of v [3]) and its exact value can be found from Eq. (1). Further, $v'(a)=-\lambda v_0$ and thus $b_{11}=\lambda v_0|c'(v_0)|$. It is easy to see that $b_{22}=D_v\Delta-\epsilon$, where Δ is the Laplacian operator. The spatial distribution of the perturbation of v can be represented as a series $\sum_{i=0}^{\infty}c_k\cos(kx)$, which gives for mode k, $\Delta=-k^2$. Therefore the condition for each mode to become unstable is $\operatorname{tr}(B)=\lambda v_0|c_v|-D_vk^2-\epsilon>0$. This indicates that the most sensitive mode corresponds to $k=0$ or when $\delta v(x)=\delta v$ is a constant. Finally for the bifurcation point D_3 we have $\operatorname{tr}(B)=\lambda v_0|c_v|-\epsilon=0$ or taking into account that $\lambda=\sqrt{\epsilon/D_v}$:

$$D_3=(c_v v_0)^2\epsilon^{-1}, \tag{3}$$

i.e., D_3 is proportional to ϵ^{-1}. This confirms results obtained in [6,7] where more complicated methods were used to analyse more general systems. To analyse the condition $\det(B)>0$ we shall find expressions for b_{12} and b_{21}. It is easy to see that $b_{12}=c'(v_0)$ and the expression for $b_{21}=\epsilon(v_0(a+\delta a)-v(a+\delta a))$, i.e., b_{21} depends on the difference between the value of v at the front of stationary spot with size $a+\delta a$, which is $v_0(a+\delta a)=v_0+(1-2v_0)\lambda\delta a$, and the value of v at distance δa from the front of stationary spot of size a, $v(a+\delta a)=v_0(1-\lambda\delta a)$. Thus $b_{21}=\epsilon(1-v_0)\lambda$ and the condition $\det(B)=b_{11}b_{22}-b_{12}b_{21}>0$ transforms into $2v_0<1$. The sign of $\det(B)$, which is positive if $v_0<0.5$, does not depend on D_v and ϵ.

To estimate D_1 we shall find conditions when the system (1), (2) has a travelling wave solution. In a similar manner to the case of a stationary spot we replace the u-profile by the rectangular wave and look for a solution $v(x-ct)=v(z)$ to the equation $D_vv''+cv'+\epsilon(u-v)=0$ under the same conditions as above except for $v(a)=v^+$ and $v(-a)=v^-$ (see Fig. 2E). The solution is $v(z)=v_0\exp[\lambda_1(z-a)]$ for $z>a$, $v(z)=v_1\exp[\lambda_2(z+a)]$ for $z<-a$ and $v(z)=1-\lambda_2\exp[\lambda_1(z+a)]/(\lambda_2-\lambda_1)+\lambda_1\exp[\lambda_2(z-a)]/(\lambda_2-\lambda_1)$ for $|z|\leqslant a$ where $\lambda_{1,2}=(-c\mp\sqrt{c^2+4\epsilon D_v})/(2D_v)$. Parameters c and a are defined by v^+ and v^- according to the following

equations: $v^+ = \lambda_2[1 - \exp(2\lambda_1 a)]/(\lambda_2 - \lambda_1)$ and $v^- = \lambda_1[\exp(-2\lambda_2 a) - 1]/(\lambda_2 - \lambda_1)$. Note that the size of wave, a, must be big enough for $v^- > v_0$ (see Fig. 2A). To find conditions for the existence of a propagating wave solution we rewrite the expression for v^- as $v^-(\lambda_2 - \lambda_1)/\lambda_1 + 1 = \exp(-2\lambda_2 a)$. Since $0 < \exp(-2\lambda_2 a) < 1$ we conclude $-1 < v^-(\lambda_2 - \lambda_1)/\lambda_1 < 0$. From the last inequality, after putting the expressions for λ_1 and λ_2 we derive $D_v\epsilon < c^2 v^-(1 - v^-)/(2v^- - 1)^2$. Since the velocity of the wave, c, can vary in a limited range and $c = O(1)$ [3] and $v^- = O(1)$ (Fig. 2A), we can expect that:

$$D_1 \propto \epsilon^{-1}. \tag{4}$$

This result was also obtained in [6] where a propagating wave solution of (1), (2) was studied using analogies with mechanical systems. Our numerical results confirm both conditions (3), (4). Moreover, according to our simulations all three threshold values for inhibitor diffusion, D_1, D_2 and D_3, separating domains R1–R4, can be approximated as linear functions of ϵ^{-1} (Fig. 1I). No analytical estimations of D_2 were reported so far, but from the linearity of $D_2(\epsilon^{-1})$ we can gain some information. As was noted before at $D_v = D_2$ the amplitude of spot pulsations, A, is equal to its mean size, S. The last seem to comply with $S \sim \sqrt{D_v/\epsilon}$ (similar to the size of a stationary spot). Thus for D_2 to be a linear function of ϵ^{-1}, the amplitude A must be proportional to ϵ^{-1}.

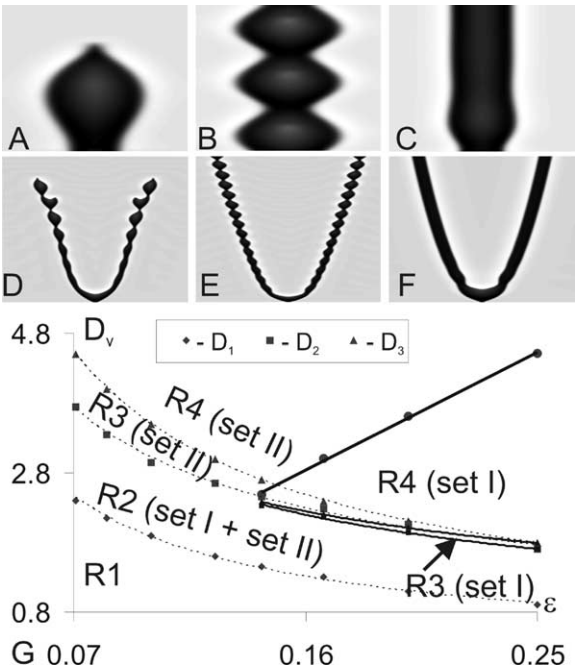

Fig. 3. A–F: time–space plots of cross-sections of radially symmetric patterns. Unstable (A, plot size 100×40, $D_v = 1.7$, $\epsilon = 0.2$), pulsating (B, 400×40, $D_v = 1.95$, $\epsilon = 0.2$) and stationary (C, 400×60, $D_v = 2.5$, $\epsilon = 0.2$) spots form set I solutions, which are similar to 1D patterns shown in Fig. 1B–D. Unstable (D, 600×320, $D_v = 2.6$), pulsating (E, 1000×280, $D_v = 3$) and asymptotically stable (F, 600×200, $D_v = 5$) rings form set II solutions. G: plane (D_v, ϵ) as divided into domains corresponding to different solutions. Transition lines between propagating waves and set II R2–R4 solutions coincide with transition lines between R1–R4 solutions in 1D-system (i.e., D_1–D_3 lines in Fig. 1I). Areas where set I R3 and R4 solutions can be initialised are located between bold lines.

4. Radially symmetric two-dimensional patterns

The next step in our study is the investigation of two-dimensional solutions of (1), (2). This study will be performed in two steps. First we focus on radially symmetric patterns. Cross-sections of these patterns can be obtained in a quasi-one-dimensional system (1), (2) where the diffusion terms are rewritten according to the transformation from Cartesian to polar coordinates, i.e., $\Delta(= \partial^2/\partial x^2 + \partial^2/\partial y^2) = \partial^2/\partial r^2 + r^{-1}\partial/\partial r$. We have found that four basic types of 1D-solutions can also be initiated in this system (shown in Fig. 1A–D). Propagating wave solutions are observed in the domain which exactly corresponds to the R1-domain in the 1D-system (Fig. 1I). The only notable difference is that the R1 solution in the quasi-1D-system is a concentric wave whose velocity, c, changes over time, or, more precisely, with its radius according to the eikonal equation, $c = c_0 - D_{\text{eff}} * k$, where k is the curvature of the wave-front; c_0 is the velocity of a planar wave, and D_{eff} is an effective diffusion coefficient, which is a function of the model parameters [9].

Similar to the 1D-system there is a domain (R2) in a parameter space of the quasi-1D-system where no stable solutions can be initiated. Two kinds of unstable patterns have been observed here (Fig. 3A, D). In the quasi-1D-system no persistent patterns like those presented in Fig. 1F–H can be initialised. The R2-domain in the quasi-1D-system coincides with the R2-domain in the 1D-system (Fig. 3G). Pulsating and stationary spots can also be initiated in the quasi-1D-system (Fig. 3G). However, the domains for these

solutions are found to be different from the R3 and R4 domains in the 1D-system. The values of D_2 and D_3 in the quasi-1D-system are smaller (borders between domains R2, R3 and R4 are shifted down) when compared with those for the 1D-system (see Fig. 3G). In addition these spots can be initiated only in the area under the linear plot $D_v(\epsilon)$ presented in Fig. 3G.

In the quasi-1D-system we have observed new kinds of solutions which do not arise in the 1D-system. These solutions are represented by concentric propagating waves which slow down over time (Fig. 3D–F). We will call these decelerating waves "expanding rings" to distinguish them from propagating waves (or R1-solutions). Considering the pattern shown in Fig. 3D as an unstable expanding ring we will describe three kinds of expanding rings: unstable, pulsating and asymptotically stationary (Fig. 3D–F). We will call expanding rings 'set II solutions' to distinguish them from 'set I solutions' shown in Fig. 3A–C and representing unstable, pulsating and stationary spots. Thus, each set contains 3 kinds of solutions, which, by analogy with 1D-solutions, we will call R2, R3 and R4 solutions. The domains where R2, R3 and R4 rings can be initiated coincide with R2, R3 and R4 domains for the 1D-system shown in Fig. 1I. Expanding rings of R2 and R3 type pulsate (Fig. 3D, E). The amplitude of these pulsations increases with increasing ring radius. R2 rings vanish due to the high amplitude of pulsations (Fig. 3D). R3 and R4 rings asymptotically stabilize over time (Fig. 3E, F). As the radius of the ring increases, the velocity of the ring expansion saturates at $c = 0$ and the amplitude of pulsations (of R3-ring) at the value of that for pulsating spots in the corresponding 1D system. Time–space plots of R3 and R4 rings (Fig. 3E, F) show that the time of expansion and the ring radius are linked by a parabolic law: t is proportional to r^2 (checked by polynomial interpolation of time–space plots of the fronts of the rings). This indicates that the eikonal equation for these rings is $c = Ak$, i.e., $c_0 = 0$ (planar waves do not propagate) and the effective diffusion $D_{\text{eff}} = -A$ is negative.

We emphasize that the domains where R3 and R4 rings can be initiated coincide correspondingly with R3 and R4 domains in the 1D-system. The domains where R3 and R4 spots can be initialised are much smaller and their borders (shown by bold lines in Fig. 3G) do not coincide with those of any domains in the 1D-system. Note that these domains contain multiple attractors. Depending on the stimulation procedure in these domains we can initialise either spots (pulsating or stationary) or rings (pulsating or asymptotically stationary) (Fig. 3G). Generally it appears that the stimulation procedure must be carefully tuned to get pulsating or stationary spots, while expanding rings represent more robust solutions.

To explain the transition between sets I and II solutions let us consider a radially symmetric stationary spot, whose u-profile is represented by the characteristic function of excited area (Fig. 2C). The v-profile in this spot is given by a solution of the cylindrical equation $D_v v_{xx} + D_v v_x/x + \epsilon(u - v) = 0$, where $u = 1$ for $|x| \leqslant a$ and $u = 0$ for $|x| > a$, $v \in C^1(-\infty, \infty)$, $v(-\infty) = v(\infty) = 0$ and $v(-a) = v(a)$. The solution is a symmetric function $v(x) = 1 + (v(a) - 1)I_0(\lambda x)/I_0(\lambda a)$ for $|x| \leqslant a$ and $v(x) = v(a)K_0(\lambda x)/K_0(\lambda a)$ for $|x| > a$, where I_0 and K_0 are modified Bessel functions and $\lambda = \sqrt{\epsilon/D_v}$. Contrary to the 1D-spot where $v(a) = v_0$ is constant, the value $v(a)$ for a 2D-spot depends on its size, namely $v(a)$ corresponds to the value v^+ in the front of 1D-wave propagating with the speed c such that $c + D_v/a = 0$ [8]. Similarly, the maximum value of the inhibitor, which is achieved at $x = 0$, $v(0) = 1 - (1 - v(a))/I_0(\lambda a)$, now depends on a and λ. According to our simulations $v(0)$ increases with a decrease of λ and there is a critical value of λ such that $v(0) = v_{\max}$. At this point the spot becomes unstable [6]. Indeed, $v(0) > v_{\max}$ causes the deformation of the spot: the medium around $x = 0$ relaxes and the spot transforms into the ring. The value of λ corresponding to $v(0) = v_{\max}$ explains the restriction for the formation of spots given by the linear plot in Fig. 3G. $\lambda = \sqrt{\epsilon/D_v}$ is constant along this line. The size of the spot along this line is also constant and corresponds to the maximal size of the stable spot in the medium.

Transition lines between stationary and pulsating spot solutions as well as between pulsating spot and unstable solutions in a quasi-1D system do not coincide with corresponding lines in a 1D-system. This can be explained by differences of the v-profiles in 1D- and quasi-1D spots. Indeed, the values $v(a)$ and $v'(a)$ on the "wall" of spot in these two cases are

different giving different values of D_3 (see Eq. (3)) for stationary spots to become unstable. A reduction of D_2 most likely has a similar nature.

5. General two-dimensional patterns

We now study general 2D-patterns arising in the system (1), (2) where the Laplacian $\Delta = \partial^2/\partial x^2 + \partial^2/\partial y^2$. The radially symmetric 2D-patterns studied in the previous section can be initiated in this system provided that they are stable. Unstable patterns, which are sensitive to noise applied to the system (and/or to anisotropy induced by the integration scheme), evolve by becoming radially asymmetric into new kinds of patterns. Thus, our next task is to study which of the radially symmetric patterns show angular instability and into what kinds of patterns do they evolve under the influence of noise. The effect of noise was modelled by additional terms $r_1(x,t)$ and $r_2(x,t)$ on the right-hand side of Eqs. (1), (2):

$$\frac{\partial u}{\partial t} = D_u \Delta u - \epsilon_u f(u,v) + r_1(x,t), \tag{5}$$

$$\frac{\partial v}{\partial t} = D_v \Delta v + \epsilon \phi(u,v) + r_2(x,t). \tag{6}$$

The terms $r_1(x,t)$ and $r_2(x,t)$ represent a white noise characterised by the amplitude and time and space steps, these values are set to 0.01, 1.0 and 2.0, respectively. Our control simulations with up to five-fold variations of these values have shown no changes in the noise-sensitivity of the original pattern, although the rate of noise driven transformations has altered significantly. Numerical investigation of the 1D-medium described by the system (5), (6) shows that:

(1) Propagating waves (R1-solution) are stable: noise applied to the system just slightly increases their velocity (the effect reported in [10]).
(2) Pulsating and stationary spots (R3 and R4 solutions) are also noise-insensitive.
(3) The noise does not alter the behaviour of vanishing waves (R2-solutions shown in Fig. 1B, E), however, persistent R2-solutions (Fig. 1F–H) can significantly be affected by noise.

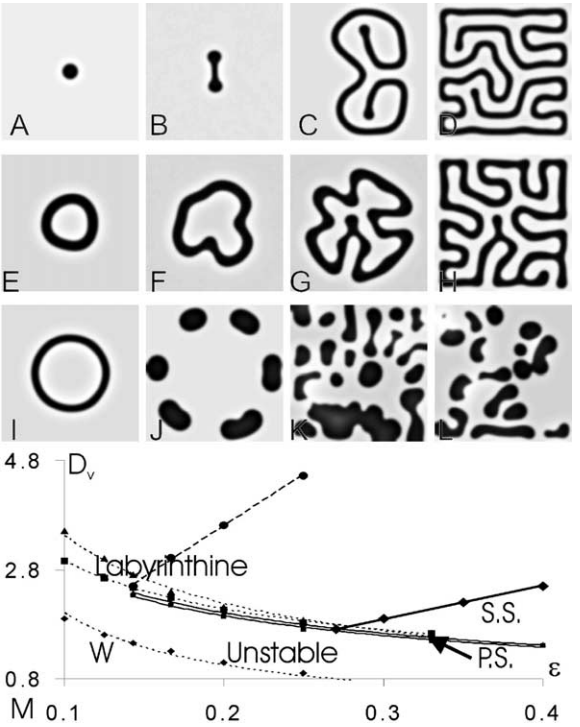

Fig. 4. Two-dimensional patterns arising in the system (1), (2). A–D: evolution of unstable stationary spot (set I R4-solution) into the labyrinthine pattern. Snapshots are taken at times 0, 200, 1000 and 3000 correspondently. E–H: transformation of an expanding ring (set II R4-solution) into the labyrinthine pattern (250, 400, 500, 1500). I–L: transformation of unstable expanding ring (set II R2-solution) into self-replicating spots (150, 300, 500, 1000). All simulations are performed in the 120×120 medium. M: plane (ϵ, D_v) as divided into domains corresponding to different 2D-solutions. A solid bold line separates stationary spots from labyrinthine patterns. All other lines are taken from Fig. 3G. Abbreviations: W propagating waves, S.S. stationary spots, P.S. pulsating spots.

Investigation of 2D-patterns shows that propagating waves and vanishing spots (i.e., R1 and set I R2 solutions) are noise-insensitive. Pulsating and stationary spots (set I R3- and R4-solutions) are stable provided that they are small. In our model medium (described by the functions $f(u,v)$ and $\phi(u,v)$) spots are stable provided that they are smaller than 16 space units and unstable otherwise. This size of the spot is achieved along the bold solid line shown in Fig. 4M, spots are stable only on the side of this line corresponding to smaller values of D_v. Under the influence of noise, unstable stationary spots transform into what is seen

as "labyrinthine patterns" (Fig. 4A–D). These transformations are slow (compared to all processes considered so far) and the final patterns are stationary. The appearance of the labyrinthine patterns varies depending on the model parameters. An increase of D_v adds more branches (free ends) in the "labyrinthine walls". A decrease in ϵ can cause division of the original spot into a few pieces (self-replication) and correspondingly the "walls of the labyrinth" will be formed by a few disconnected lines.

Expanding rings (set II R3–R4 solutions) are also noise sensitive and transform into the labyrinthine patterns (Fig. 4E–H). This transformation starts only when their expansion velocity is small enough (i.e., it might take a while before the ring expands, slows down and starts to deform). Vanishing expanding rings (R2 solutions) generally disappear too quickly to show any noise sensitivity. However, R2-solutions close to the boundary with the R3 domain can exhibit a self-replicating phenomenon: an expanding ring can divide into a few spots, each of which can give rise to new spots and so on (Fig. 4I–L). These self-replicating spots can

(a) all vanish over time (the medium relaxes into the homogeneous state);
(b) elongate and give rise to a labyrinthine pattern formed by disconnected "walls"; and
(c) show chaotic and endlessly oscillating patterns.

6. Discrete systems

In this section we consider phenomena observed in the discrete system described by Eqs. (1), (2). We assume that diffusion coefficient D_u is small compare to the kinetics term $f(u, v)$ and will consider patterns arising in this system. To check the effect of discreteness on the location of domains in the 1D-system we have produced plots of D_1/D_u, D_2/D_u, and D_3/D_u versus D_u (Fig. 5A). One can see that these critical values start to change and all drop when the value of D_u gets small enough ($D_u < 0.5$) and discreteness starts to play a role. The types of 1D-patterns observed in discrete systems are the same as in continuous systems. However, we have observed a few phenomena specific to discrete systems:

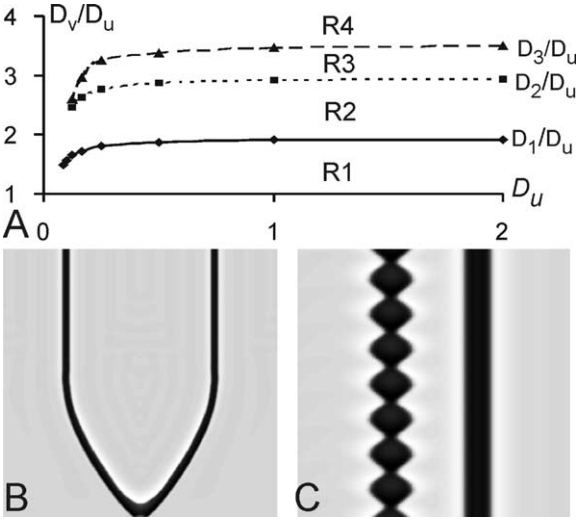

Fig. 5. A: location of the domains R1, R2, R3 and R4 on the plane (D_u, D_v/D_u). B: in a discrete system when $D_u < 0.15$ R2 and R3 domains are missing and propagating waves can transform directly into stationary spots. C: pulsating and stationary spots can be observed on the same point in parameter space. B: size of the plot 200×120, $D_u = 1/8$, $D_v/D_u = 1.7$; C: 500×40, $D_u = 1/8$, $D_v/D_u = 2.5$.

(1) A significant decrease of D_u can result in the loss of pulsating wave solutions, which can be restored by simultaneous reduction of ϵ. This is similar to what we see in Fig. 1I: the lines for D_2 and D_3 intersect at $\epsilon = 1/3$ and no pulsating spots can be observed when $\epsilon \geqslant 1/3$.
(2) Transitions between solutions become more complicated. For example, at $D_v = D_1$, propagating waves can directly transform into stationary spots (Fig. 5B).
(3) Different patterns can be observed in the same medium. Fig. 5C shows stationary and pulsating spots coexisting in the same medium (this coexistence is not due to the interactions of spots since a single pulsating spot or a single stationary spot can be initiated in this medium).

All results concerning quasi-1D- and 2D-patterns are qualitatively the same in discrete and continuous systems. Both sets of radially-symmetric solutions are observed in a discrete system, although stationary spots can now be initiated in a wider range of model parameters. We have found a new radially-symmetric pattern which can be initiated in a discrete

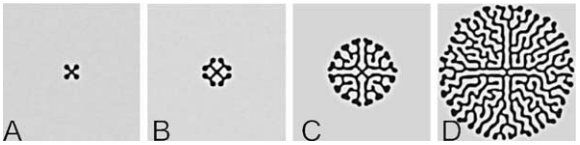

Fig. 6. Formation of a streaming pattern in a 2D discrete system. Snapshots at times $t = 100$ (A), $t = 300$ (B), $t = 500$ (C) and $t = 1000$ (D) are shown. Size of the medium 120×120, $D_u = 1/8$, $D_v = 5/8$, $\epsilon = 0.25$.

system. This pattern is observed when the diffusion of the activator is very small ($D_u < 0.1$) and represented by a stationary (not expanding) ring. Noise sensitivity of 2D-patterns in discrete systems is very similar to that in continuous systems, although the appearance of labyrinthine patterns can be very different. Fig. 6 shows the evolution of a typical labyrinthine pattern in a discrete system. This pattern can be considered as a "streaming pattern" growing from the centre. A decrease in D_u and an increase in the difference between D_u and D_v transforms the shape of labyrinthine patterns so that they look more and more like snowflakes.

7. Discussion

In this Letter we have studied 1D- and 2D-solutions arising in the excitable system (1), (2) and established links between them. Four basic types of 1D-solutions (Fig. 1A–D) have been reported and studied earlier [3–7]. We have explored different R2 type persistent patterns (Fig. 1F–H) and identified their relationships with other types of 1D-patterns. The transitions caused by instability of propagating waves and stationary spots in a 1D-medium (represented by D_1 and D_3 lines in Fig. 1I) are relatively well-studied [5–7]. Here we have examined numerically how transition points depend on model parameters. To explain these observations we have presented a simple model, which allowed us to make analytical estimations for the bifurcation values D_1 and D_3.

2D-patterns such as stationary spots (Fig. 4A), self-replicating stripes and spots (Fig. 4D, F) and labyrinthine patterns (Fig. 4B, E) have also been reported and studied earlier [11–14]. However the transitions between them are mostly unknown [15]. Our study of radially-symmetric 2D patterns was designed to establish a link between 1D- and 2D-patterns and consequently to explore transitions between 2D-patterns. Analysing different types of radially-symmetric 2D-patterns, we divided them into two sets. Set I is represented by patterns which are exactly the same as R1–R4 type patterns in 1D-medium. Set II solutions represented by expanding rings corresponding to R2–R4 solutions in 1D-medium (Fig. 3D–F). We have found that the transition points between set II solutions are exactly the same as those between the corresponding 1D-solutions. The domains where set I solutions can be initialised are smaller, and their transition points do not coincide with any transition points between 1D-solutions.

To study general 2D-patterns we assumed that these patterns are derivations from radially-symmetric patterns affected by noise and instability. We have found that pulsating and stationary spots can exist in a 2D-medium provided that they are small. Large spots are sensitive to noise and evolve into labyrinthine patterns (Fig. 4A–D). Pulsating and expanding rings are found to be always noise-sensitive. They also evolve into labyrinthine patterns (Fig. 4E–H). Vanishing expanding rings (set II R2-solutions) most commonly vanish but sometimes transform either into self-replicating spots (Fig. 4I–L) or into labyrinthine patterns.

The types of patterns and the transitions between them observed in discrete systems are mostly the same as those in continuous systems. Notable phenomena specific to discrete systems are the coexistence of different types of solutions (Fig. 5C) and the formation of streaming patterns (Fig. 6). Streaming patterns have previously been found in a framework of cellular-automata models [16,17], where their formation was considered as a particular case of diffusion-limited aggregation.

We believe that we have explored all 1D- and 2D-patterns which can be initiated in the modified Fitz-Hugh–Nagumo system (1), (2). In addition we have identified all transitions and links between them. The present study can be extended by considering patterns and their transitions in other models (e.g., Gierer–Meinhardt, Turing pre-pattern) and other classes of systems (oscillatory, trigger). On the other hand the results presented here give rise to many problems in transitions between solutions and the stability of solutions which may be addressed analytically.

Acknowledgements

We wish to acknowledge Prof. Mark Chaplain, Dr. Sandy Anderson and Dr. Fordyce Davidson for helpful discussions and comments on the manuscript.

References

[1] F.H. Busse, S.C. Muller (Eds.), Evolution of Spontaneous Structures in Dissipative Continuous Systems, Springer-Verlag, Berlin, 1998.
[2] M.A.J. Chaplain, G.D. Singh, J.C. McLachlan (Eds.), On Growth and Form: Spatio-Temporal Pattern Formation in Biology, Wiley, Chichester, 1999.
[3] R. Fitzhugh, in: H. P Schwan (Ed.), Biological Engineering, McGraw–Hill, New York, 1969.
[4] H. Meinhardt, A. Gierer, Bioessays 22 (2000) 753.
[5] B. Vasiev, A. Panfilov, R. Khramov, Phys. Lett. A 192 (1994) 227.
[6] B.S. Kerner, V.V. Osipov, Sov. Microelectronics 6 (1977) 337;
B.S. Kerner, V.V. Osipov, Sov. Microelectronics 12 (1983) 512;
B.S. Kerner, V.V. Osipov, Autosolitons: A New Approach to Problem of Self-Organisation and Turbulence, Kluwer, Dordrecht, 1994.
[7] Y. Nishiura, M. Mimura, SIAM J. Appl. Math. 49 (1989) 481.
[8] J.P. Keener, SIAM J. Appl. Math. 46 (1986) 1039.
[9] A.V. Panfilov, J.P. Keener, SIAM J. Appl. Math. 55 (1995) 205.
[10] I. Sendina-Nadal, A.P. Munuzuri, D. Vives, V. Perez-Munuzuri, J. Casademunt, L. Ramirez-Piscina, J.M. Sancho, F. Sagues, Phys. Rev. Lett. 80 (1998) 5437.
[11] K.J. Lee, W.D. McCormick, J.E. Pearson, H.L. Swinney, Nature 369 (1994) 215.
[12] K.J. Lee, H.L. Swinney, Phys. Rev. E 51 (1995) 1899.
[13] P.W. Davies, P. Blanchedeau, E. Dulos, P. De Kepper, J. Phys. Chem. A 102 (1998) 8236.
[14] W.N. Reynolds, S. Ponce-Dawson, J.E. Pearson, Phys. Rev. E 56 (1997) 185.
[15] W.N. Reynolds, J.E. Pearson, S. Ponce-Dawson, Phys. Rev. Lett. 72 (1994) 2797.
[16] E. Ben-Jacob, I. Cohen, H. Levine, Adv. Phys. 49 (2000) 395.
[17] E. Ben-Jacob, Contemp. Phys. 38 (1997) 2797.